Water Research 150 (2019) 340–348

Contents lists available at ScienceDirect

Water Research

journal homepage: www.elsevier.com/locate/watres

Bioenergy generation and degradation pathway of phenanthrene and anthracene in a constructed wetland-microbial fuel cell with an anode amended with nZVI

Junfeng Wang [a], Xinshan Song [b, *], Qusheng Li [a], Heng Bai [b], Congyun Zhu [a], Baisha Weng [c], Denghua Yan [c], Junhong Bai [d]

[a] School of Environment, Jinan University, Guangzhou, 510632, Guangdong, China
[b] College of Environmental Science and Engineering, Donghua University, Shanghai, 201620, China
[c] China Institute of Water Resources and Hydropower Research, Beijing, 100038, China
[d] School of Environment, Beijing Normal University, Beijing, 100875, China

ARTICLE INFO

Article history:
Received 21 July 2018
Received in revised form
12 November 2018
Accepted 27 November 2018
Available online 30 November 2018

Keywords:
Polycyclic aromatic hydrocarbons
Bioelectricity generation
Phytoextraction and phytotransformation
Nitrogen removal
Bacterial community distribution

ABSTRACT

The frequent occurrence of polycyclic aromatic hydrocarbons (PAHs) in aquatic environments is of great concern because of their teratogenicity, toxicity, carcinogenicity, and mutagenicity to plants, animals and human beings. In this study the bioelectricity generation, biodegradation, phytoextraction and substrate adsorption of phenanthrene and anthracene in a constructed wetland-microbial fuel cell (CW-MFC) were investigated with an anode electrode amended with or without biochar-nZVI. During a 182-day operation period, the average removal efficiency for phenanthrene and anthracene ranged from 88.5% to 96.4%. The concentration of phenanthrene in roots, stems and laminas of *T. orientalis* was 14.9, 3.9 and 2.3 ng g^{-1} respectively, while that of anthracene was 22.2, 3.1 and 1.3 ng g^{-1}, respectively. In addition, the application of nZVI was conducive to bioelectricity generation and organic compound degradation in the CW-MFC reactor. The distribution of the bacterial community indicated that the relative abundance of *Bacillus*, *Paludibacter*, *Desulfovibrio* and *Lactococcus* with a degradation capability for refractory organics was significantly increased. Especially the genus *Bacillus* for excreting catalase became more abundant. The results of our study indicate how to promote bioelectricity generation and biodegradation of refractory organic compounds in a CW-MFC by improving the culture conditions for bacteria.

1. Introduction

Polycyclic aromatic hydrocarbons (PAHs) occur frequently in aquatic environments such as surface and ground water and even in effluents of wastewater treatment plants (WWTPs) (Hamdan et al., 2017). Although the concentrations of these compounds are at trace level (ng L^{-1} to μg L^{-1}) (Qi et al., 2013), they are considered to pose a serious threat on plants, animals and humans (Goldman et al., 2001; Pašková et al., 2006). Hence, PAHs are of increasing concern because of their teratogenicity, toxicity, carcinogenicity, and mutagenicity (Haritash and Kaushik, 2009; Yu et al., 2017). Owing to their persistence and stability, the process of volatilization, chemical oxidation, and photo-oxidation usually do not meet the requirements of environmental protection under natural conditions (Haritash and Kaushik, 2009; Wild and Jones, 1995). In addition, different congeners of the same group (PAHs) can interact with each other, consequently, reduce their removal efficiency (Lei et al., 2007). Therefore, developing efficient methods to control PAH pollution in aquatic environments is an important issue for environmental protection.

A constructed wetland-microbial fuel cell (CW-MFC), which utilizes natural processes to generate bioelectricity and promotes the removal efficiency of contaminants within a controlled environment, has been considered to be a low-cost, easily to maintain and environmentally friendly technology for wastewater treatment (Wang et al., 2016; Yadav et al., 2012). There are many successful tests using a CW-MFC for the biodegradation of azo dye products and swine slurry remains (Doherty et al., 2015a; Fang et al., 2015). Although these work have demonstrated that the use of a CW-MFC can significantly enhance the removal efficiency of contaminants by

* Corresponding author.
E-mail address: newmountain@dhu.edu.cn (X. Song).

https://doi.org/10.1016/j.watres.2018.11.075
0043-1354/

oxidation coupled with electron transfer to the anode by an adapted microbial population (Doherty et al., 2015b). The effect of these factors on the removal performance of PAHs by a CW-MFC has never been reported. In addition, most of the reported work on CWs for PAH treatment is related to the removal efficiency of these contaminants. Since CWs comprise of water, plants, substrate and microorganisms, it is essential to achieve a comprehensive understanding of the mechanisms involving phytoextraction, phytotransformation, substrate adsorption and biodegradation in CWs during wastewater treatment.

In a CW-MFC the metabolic functions of microorganisms play an important role in contaminant removal and electron transfer. It has been shown that the increase of the abundance of electrochemically active bacteria (EAB) like *Pseudomonas*, *Dechloromonas*, *Rhodopseudomonas* or *Desulfuromonas* may result in an enhancement of bioelectricity generation in a CW-MFC (Corbella et al., 2015; Wang et al., 2016). In addition, many studies demonstrated that the bioenergy output from MFCs with mixed microbial cultures is higher than the one with pure cultures (Nevin et al., 2008; Rabaey and Verstraete, 2005). One possible cause may be that synergistic interactions promote the electron flow among the microbial community causing an increased bioelectricity generation (Corbella et al., 2015). In addition, it was observed that the use of zero valent iron (ZVI) in a MFC system can increase electricity generation and biodegradation of organic compounds because of its function as electron donor causing a reduction of the of organic compounds (Cai et al., 2018; Zhang et al., 2011). These results suggest that an anode amended with nano ZVI (nZVI) might improve the degradation of organic compounds as well as electricity production.

In this study, phenanthrene and anthracene were selected as target PAHs. The control group and the CW-MFC with an anode amended with nZVI were used to investigate their performance in biodegradation, phytoextraction and substrate adsorption of phenanthrene and anthracene. We hypothesize that: i) nZVI affects the biodegradation and phytoextraction of phenanthrene and anthracene during wastewater treatment; ii) an increased bioelectricity generation of a CW-MFC anode amended with nZVI will promote the nitrogen removal of the wastewater; iii) the microbial community will adapt to the nZVI located anode in a CW-MFC and change its composition.

2. Materials and methods

2.1. Preparation of Biochar-Mt-nZVI

Montmorillonite-nZVI (Mt-nZVI) was prepared by reducing $FeSO_4 \cdot 7H_2O$ to zero valent iron using sodium borohydride ($NaBH_4$) reduction (Huang et al., 2014; Zhang et al., 2010). Firstly, 24.88 g of $FeSO_4 \cdot 7H_2O$ were dissolved in an ethanolic solution (200 mL) at a volume ratio of 1 (water):4 (ethanol). Then 20 g Mt were added and stirred for 0.5 h. Afterwards, $NaBH_4$ solution (50 mL) was added to the Mt-nZVI under continuous stirring at a mol ratio of $1(Fe_2^{+}):3(BH_4^{-})$. Finally, the mixture was stirred for another 0.5 h under the protection of N_2. Mt-nZVI was washed with deionized water for several times and dried at −40 °C for 24 h in a lyophilizer. Meanwhile, biochar was added into 50 mL anoxic deionized water and heated in a water-bath (50 °C). Then it was placed for 1 h to discharge the bubble. Finally, the Mt-nZVI and an anoxic $CaCl_2$ solution (4%) were added to the above solution and stirred for about 1 h. The next step in the preparation of Biochar-Mt-nZVI was repeated according to the above-mentioned processes. The final products were used as the amendment material to embed in the space between of anode electrode. The surface area, SEM and XRD parameters are presented in Table S1 and Fig. S1.

2.2. Reactor construction, inoculation and operation

The schematic diagram of a CW-MFC reactor (height 52 cm; internal diameter 16 cm; material polyvinyl chloride) is shown in Fig. 1. Foamed nickel (FN), foamed nickel amended with nZVI (FN-nZVI), carbon fiber felt (CFF) or carbon fiber felt amended with nZVI (CFF-nZVI) were selected as anode materials. The cathode materials were similar with to corresponding anodes without any emendation. The diameter of each electrode was 10 cm and the weight of Biochar-Mt-nZVI in the FN-nZVI and in the CFF-nZVI reactor was 3.2 g. The distance of the electrodes was 35 cm. They were connected with an external electrical resistor (1000 Ω). All units were filled with uniform quartz sand with an average particle size of 2–4 mm and a porosity of 29.2%. After macro-nutrients and Hoagland's trace elements had been added for one month, *Typha orientalis* (*T. orientalis*) was respectively planted into the CW-MFCs with an initial density of 6 plants per unit. The CW-MFC were inoculated with a volume of 2.0 L active sludge, collected from a wastewater treatment plant in Shanghai Songjiang area, which has been diluted with tap water. Synthetic municipal wastewater was used to adapt the microorganisms and wetland plants for about one month. During inoculation and operational periods, synthetic wastewater was fed into the CW-MFCs at the top and collected from a perforated collection pipe placed 7 cm above the bottom of reactor. All CW-MFCs were operated in a fed-batch mode with a hydraulic retention time (HRT) of 2 d.

2.3. Preparation of synthetic wastewater

The composition of synthetic wastewater is as follows: $C_6H_{12}O_6 \cdot H_2O$, KH_2PO_4, $Na_2HPO_4 \cdot 12H_2O$, NH_4Cl, $NaNO_3$, CH_3COONa, $MgCl_2 \cdot 6H_2O$, $ZnCl_2$, $CaCl_2$, $CuSO_4 \cdot 5H_2O$, $FeCl_3$ and H_3BO_3. During the operational period, 1 mL phenanthrene (5 g L^{-1}) and anthracene (5 g L^{-1}) acetone solution was added to 30 L synthetic wastewater. The chemical oxygen demand (COD), NH_3-N, nitrate, phenanthrene and anthracene concentrations in the influent were 211.9,15.0, 38.9, 0.17 and 0.17 mg L^{-1}, respectively. The average conductivity and pH of influent water were 670.1 ± 50.0 μS cm^{-1} and 7.50 ± 0.12, respectively.

2.4. Sampling and analytical methods

Influent and effluent samples were collected at the feeding time

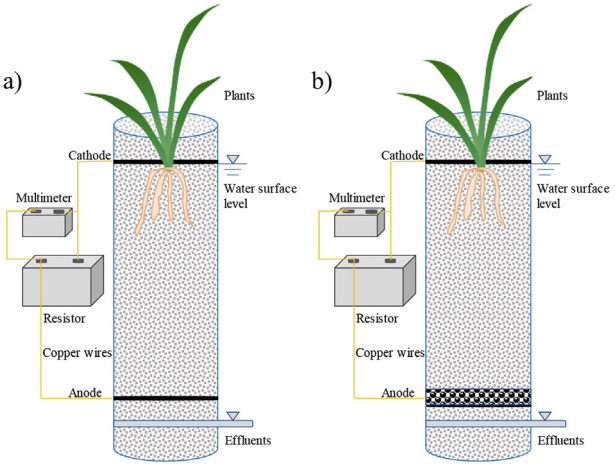

Fig. 1. The schematic diagram of CW-MFC reactor: a) CW-MFC with FN and CFF as anode material; b) the FN and CFF associated with nanoscale zero-valent iron as anode material in CW-MFC.

(9:00 a.m.) in each HRT's cycle. Dissolved oxygen (DO) concentration, pH and temperature were determined using a multi-parameter water quality monitor (HQ40d, Hach). The conductivity of influent and effluent was measured using a digital portable meter (AP-2, HM, South Korea). The concentration of NH_3-N and COD was measured with the HI 93733 Ammonia ISM (Hanna, Italy) and DR 900 (Hach, USA) with the corresponding reagents according to their special cautious. The nitrate concentration was determined with an UV-vis spectrophotometer. The fluctuating voltage across the external electrical resistor of each reactor was recorded using a digital multimeter (Hangzhou Bright Technology Co. Ltd., China) each 2 min. At the middle and at the end of the operational periods, the polarization curve of each system was determined by the variation of the external electrical resistor from 50 to 80000 Ω. Phenanthrene and anthracene concentrations of influent and effluent samples were determined according to the standard method GB/T 26411-2010 (China) for the determination of 16 PAHs in seawater by GC-MS (Shimadzu, Japan). During the operational period, 100 mL effluent samples were collected in each HRT cycle. Each ten samples were pooled and the resulting mixed solution to analyze the concentrations of phenanthrene and anthracene. In addition, to analyze the function of phytoextraction and substrate adsorption, phenanthrene and anthracene concentrations of root, stem and lamina (dry weight of each part: 1 g) of the wetland plants and in quartz sand (50 g) of each reactor were analyzed at the end of experiment, extraction by ultrasound at 25 °C, 100 W power, extractant n-hexane.

2.5. High throughput sequencing analysis

The biofilm samples of the anodes were collected at the end of the experiment. All samples were placed in a conical bottle and then centrifuged at 200 rpm for about 12 min. After that, the OMEGA soil DNA kit was used to extract DNA. The hypervariable regions of V4-V5 were amplified with the universal primers 515F (5′- GTGCCAGCMGCCGCGG-3′) and 907R (5′- CCGTCAATTCMTTTRAGTTT-3′) according to previous report (Wang et al., 2016). The PCR amplification and high-throughput sequencing analysis was done by Personal Biotechnology Co., Ltd, with an Illumina Miseq platform (Shanghai, China). To ensure high-quality sequence reads, the data were denoised and eliminated, if homopolymers exceeded 150 base pairs (bp) or were shorter than 8 bp, containing ambiguous bases and chimera sequences. All similar high-quality reads were clustered into operational taxonomic units (OTUs) with a similarity threshold value of 97%.

2.6. Statistical analysis

The characteristics of bioelectricity generation (power density, current density and coulombic efficiency) of each CW-MFC reactor was evaluated according to previous studies (Logan, 2008). The analysis of variance (ANOVA) with the LSD test (SPSS 22.0) was used to evaluate the difference of water parameters in effluents collected from the CW-MFC reactors with $p < 0.05$ as the significance level. A heat map of the microbial community at the genus level was generated using the R software (version 3.3.2) to visualize the differences and the similarities in the community composition based on the distance matrix.

3. Results and discussion

3.1. Pollutant removal and bioelectricity generation

Data in Fig. 2 show the effluent temperature, COD removal performance and voltage output of the CW-MFC reactors with FN, FN-nZVI, CFF or CFF-nZVI as anodes. In general, the temperature of the effluent ranged from 29.4 (summer) to 9.5 (winter) °C. The COD concentration of the effluents collected from the four reactors was 77.9 ± 16.4, 68.4 ± 12.7, 59.6 ± 10.6 and 50.7 ± 8.8 mg L^{-1}, respectively. The corresponding removal efficiency values were $63.3 \pm 7.2\%$, $67.8 \pm 5.7\%$, $71.9 \pm 4.7\%$ and $76.1 \pm 3.9\%$. An apparent difference in COD removal efficiency was obtained among the four reactors ($p < 0.05$). The average voltage output of FN, FN-nZVI, CFF and CFF-nZVI reactor during the 182-day operation period was 313 ± 28, 330 ± 36, 376 ± 34 and 425 ± 37 mV, respectively. The increase in bioelectricity generation could be concluded into: i) the addition of nZVI in the CW-MFC enhanced the average voltage output by 6.0 up to 13.0% ($p < 0.05$); ii) the bioenergy production in the CW-MFCs with CFF as anode was nearly 20.0% higher than that of the CW-MFC with FN as anode material ($p < 0.05$); iii) the average voltage of the CW-MFC was temperature dependent: in summer (June-Sep., average temperature: 26.3 ± 1.7 °C) 12.3–16.9% higher than in winter (Oct.- Dec., average temperature: 18.5 ± 4.5 °C) ($p < 0.05$).

These results indicate that the temperature and the modification of the anode material are critical factors for the performance with regard to pollutant removal and bioelectricity generation. The decline of the temperature from summer to winter had a direct effect on the production of bioenergy and on the contaminant removal, which is in agreement with our previous studies (Wang et al., 2017b). The enzyme activity of microbial population in the summer season was higher than in the winter season because average temperature decreased from 26.3 to 18.5 °C. In addition, the use of nZVI had an influence on environmental conditions such as pH and ORP, which regulate the metabolic activity of the EAB and of the anaerobic digestion (Cai et al., 2018). It has been reported that nZVI is conducive to the activity of enzymes producing acetic acid. The introduction of nZVI into the reactor resulted in enhancement of an easy-to-use metabolic substrate production around the anode (Liu et al., 2012; Yang et al., 2017). Due to the enhancement of acetic acid production and enzyme activity, the bioelectricity generation in CW-MFCs with nZVI amended anodes showed a significant increase. A similar study with a MFC also demonstrated that the application of nZVI anode promotes pollutant removal and enhances bioenergy production (Cai et al., 2018). Although the bacterial community on the anode (FN and CFF) was a slightly different in composition after 182-day operation (section 3.4), the effect of nZVI on the improvement of environmental conditions (pH and ORP), enzymes activity and electron transfer was similar (Harada et al., 2016).

The power density, current density and polarization curves obtained for the four reactors in the summer or winter seasons are presented in Fig. 3. In summer, the maximum power and current densities of the four CW-MFC reactors follow the order: FN < FN-nZVI < CFF < CFF-nZVI. The highest power density of 26.0 mW m^{-2} was measured for the CW-MFC with CFF-nZVI as anode. The peak current densities of the four reactors were 76.4, 81.5, 84.1 and 94.3 mA m^{-2}, respectively. However, during the winter season the maximum power and current densities decreased concomitant with the reduced temperature similar to previous studies (Villasenor et al., 2013; Wang et al., 2017b). The peak power density of the four reactors were 10.2, 10.9, 16.2 and 20.6 mW m^{-2}, respectively. The current density of the four systems had the following order: FN < FN-nZVI < CFF < CFF-nZVI. The highest power density of a CW-MFC was in the summer season in general between 21.6% and 29.8% higher than in the winter season. The nZVI embedded in the anode material significantly promoted the power density of the CW-MFC system. In addition, the coulombic efficiencies were 0.3%, 0.3%, 0.4 and 0.4% for the four reactors, respectively.

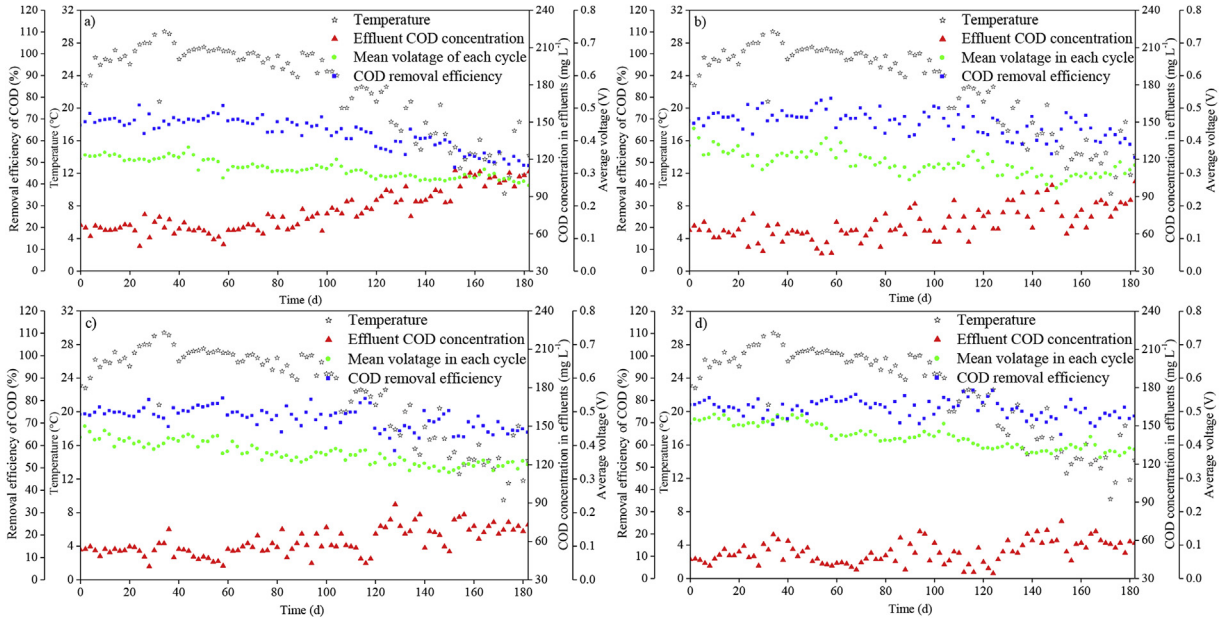

Fig. 2. The effluent temperature, COD removal performance and voltage output of CW-MFC reactor with FN (a), FN-nZVI (b), CFF (c) and CFF-nZVI (d) as the anode.

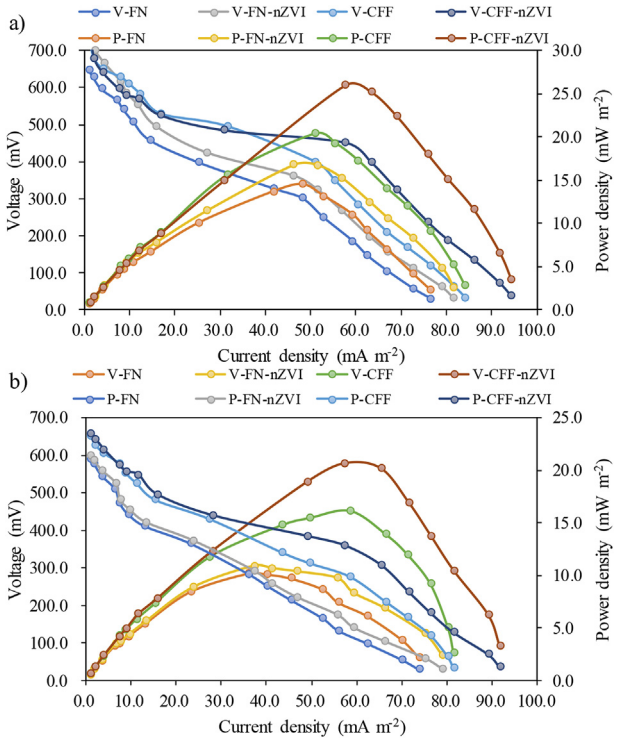

Fig. 3. The polarization curves of FN, FN-nZVI, CFF and CFF- nZVI reactors in summer or winter season: a) summer season; b) winter season.

Comparing the power density, current density and coulombic efficiency of the classic MFCs, these parameters of CW-MFC presented in a relatively lower level because of the lower efficiency of mass transfer under fed-batch mode (Cheng et al., 2006) and electron acceptors (nitrate) contained in the influent (Wang et al., 2017b). It has been reported that nitrate and ammonia could produce nitrous oxide under the chemical-denitrification effect of Fe^{2+} (Fanning, 2000). Therefore, nitrate contained in influent inhibited a higher bioelectricity generation of the CW-MFC reactor. In addition, the volume ratio of electrode biofilm to the anode in the CW-MFC was significantly lower than the one in a classic MFCs (Liu et al., 2014; Oon et al., 2017). Another cause may be the competition between EAB and other microorganisms for oxidizable organic matter in a CW-MFC system (Logan et al., 2006). During the metabolism of organic matter the syntrophic interactions between EAB (*Dechloromonas*) and hydrogenotrophic methanogens are well known (Lu et al., 2015). However, our previous study had indicated that the acetpclasic and the hydrogenotrophic methanogens played an critical role in the formation of anaerobic sludge under low and high organic loading rates (Yang et al., 2017). Therefore, the reduced concentration of organic matter in the influent may have caused that syntrophic interactions between EAB and hydrogenotrophic methanogens became inefficient and consequently the voltage output and coulombic efficiency in the CW-MFC decreased.

3.2. Degradation pathway for phenanthrene and anthracene

The biodegradation, phytoextraction and substrate adsorption of phenanthrene and anthracene in a CW-MFC are displayed in Fig. 4. With a concentration of 0.17 mg L^{-1} in the influent the removal efficiency for phenanthrene in the four reactors was 88.4 ± 2.9%, 93.6 ± 1.6%, 93.6 ± 1.6% and 95.3 ± 0.9%, respectively. The removal rates for anthracene were 92.5 ± 1.2%, 95.2 ± 1.0%, 95.8 ± 1.5% and 96.5 ± 1.5%, respectively. After 182-day operation the concentrations of phenanthrene in roots, stems and laminas of *T. orientalis* were 14.9, 3.9 and 2.3 ng g^{-1}, respectively, and that of anthracene were 22.2, 3.1 and 1.3 ng g^{-1}, respectively. In the substrate of the CW-MFC the concentration for phenanthrene and anthracene were 8.7 and 8.0 ng in 100.0 g quartz sand.

In our previous study, we assessed the distribution and metabolic function of the bacterial community around roots of *T. orientalis* (Wang et al., 2017a). Here we focus on the effect of nZVI on the biodegradation and phytoextraction of phenanthrene and anthracene at the anode in CW-MFCs. In the FN-nZVI and the CFF-nZVI reactor, the relative abundance of *Bacillus*, *Paludibacter*, *Desulfovibrio* and *Lactococcus* increased significantly during operation (section 3.4). Among these microorganisms *Bacillus*,

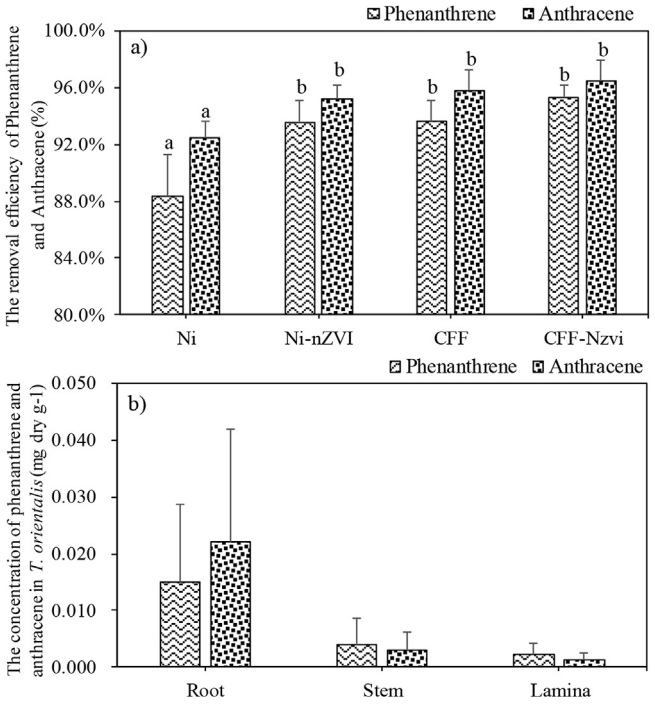

Fig. 4. The removal efficiency of Phenanthrene and Anthracene in CW-MFC (a) and the phytoextraction and phytotransformation of Phenanthrene and Anthracene in the roots, stems, and laminas of *T. orientalis* (b).

belonging to the phylum *Firmicutes*, produce the enzyme catalase under aerobic conditions (Baron, 1996). This enzyme also is considered to be involved in the biodegradation of aromatic compounds (Baran et al., 2004; Kocabas et al., 2008). The co-enriched *Paludibacter*, *Desulfovibrio* and *Lactococcus* are known to have a high capacity to remove refractory organic compounds under anaerobic conditions (Baxter-Plant et al., 2004; Rijnen et al., 1999; Yun et al., 2017). It has been reported that bacteria of the genus *Desulfovibrio* can be used to remove aromatic compounds from wastewater, since they use H_2 as electron donor (Rijnen et al., 1999). *Bacillus* and *Desulfovibrio* may contribute to the oxidation and reduction of nZVI (Volbeda et al., 1995). Bacteria of the genus *Pseudomonas* possess the capability to degrade phenanthrene and anthracene. Although the relative abundance of the latter in CW-MFCs with CFF-nZVI as anode material increased by 6.0% compared with a CFF reactor, no abundance variation was observed in the FN and FN-nZVI reactors. One possible reason may be a different effect of nZVI in FN and CFF system on the adaption of the microflora. Clear is, however, that the use of nZVI to amend the anode is conducive to the biodegradation of phenanthrene and anthracene.

Plants in wetland play a positive role in the removal of organic and inorganic contaminants from wastewater (Li et al., 2016). The potential of phenanthrene and anthracene to be taken up by the roots and their phytotransformation by *T. orientalis* were assessed by the contaminant concentrations in the roots, stems and laminas. Apparently, the plants root possessed the main uptake capacity for phenanthrene and anthracene, similar results has been obtained previously for ibuprofen remove (Li et al., 2016). However, compared with the biodegradation ability of microorganisms, these compounds removed by plants became an inefficient process, which may be caused by the main process of organic compounds removal by *T. orientalis* was carried out in an indirect effect, such as promoting the abundance of plant growth promoting bacteria (Gregoire et al., 2009; Lv et al., 2016). Although an uptake of refractory organic matter by the plant roots was limited, some phytotransformation was observed in the stems and laminas of *T. orientalis* (Pilon-Smits, 2005). For the latter activities endophytic microorganisms are probably responsible (Li et al., 2016). However, the fast biodegradation by microorganisms and defense mechanisms of plants against microbial pathogens protected *T. orientalis* (Robert and Friml, 2009). A significant low adsorption capacity for the contaminant was obtained for quartz sand in a CW-MFC. It clearly indicates that the biodegradation ability of microorganisms was possible for the quick removal of phenanthrene and anthracene. In addition, an important metabolic intermediate ([1,2-Benzenedicarboxylic acid, bis(2-methylpropyl) ester]) (Fig. S2) of the degradation process was detected in the root and stem samples of *T. orientalis*. Such finding indicates most probably that *T. orientalis* is able to do phytoextraction and phytotransformation of organic matter in wastewater treatment. However, the metabolism of these compounds in the tissues of the plant requires further research.

3.3. Nitrogen removal

Data for NH_3-N and nitrate concentrations in influents and effluents are given in Fig. 5. In general, a stable removal performance for NH_3-N and nitrate was obtained in the CW-MFCs. The average concentrations of NH_3-N in the effluents of the four reactors were 7.5 ± 1.9, 6.1 ± 1.8, 7.2 ± 2.0 and 5.1 ± 1.3 mg L^{-1}, respectively. Obviously, the NH_3-N removal efficiency for the CW-MFC with an anode amended with nZVI was significantly higher than that for the corresponding CW-MFC system ($p < 0.05$). Notably, with the decrease of the temperature in the winter season the NH_3-N concentration of the effluents in the four CW-MFC reactors ranged from 3.0 to 4.4 mg L^{-1}. Results of the linear regression analysis indicate that the NH_3-N removal efficiency increased, if the DO concentration of effluents ranged from 0.3 to 1.2 mg L^{-1}: i) $Y = 45.02X+21.98$ ($R^2 = 0.93$, FN); ii) $Y = 44.68X+31.51$ ($R^2 = 0.90$, FN-nZVI); iii) $Y = 39.78X+26.60$ ($R^2 = 0.88$, CFF); and iv) $Y = 19.42X+53.61$ ($R^2 = 0.95$, CFF-nZVI), where X and Y mean the DO concentration of effluent samples and NH_3-N removal

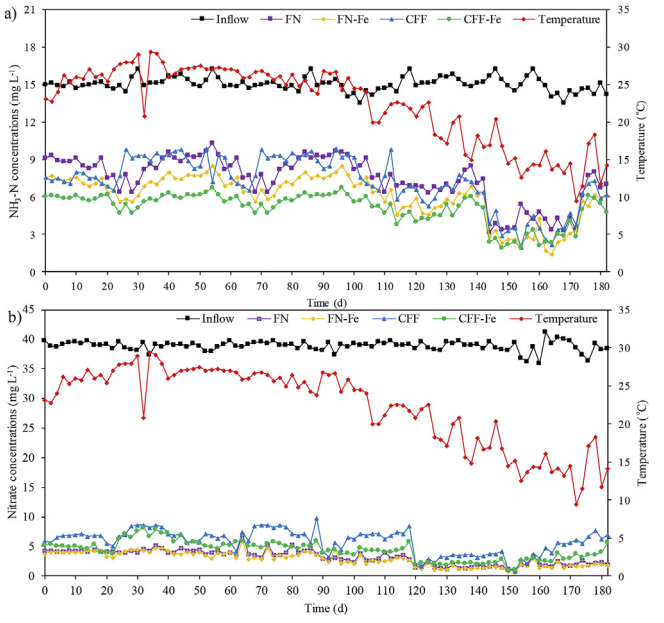

Fig. 5. The removal performance of NH_3-N (a) and nitrate (b) of FN, FN-nZVI, CFF, and CFF- nZVI reactor.

efficiency, respectively. As shown in Fig. 5(b), the nitrate concentration in the effluent samples of the four reactors were 3.2 ± 1.2, 2.9 ± 1.2, 5.9 ± 2.0 and 4.4 ± 1.6 mg L^{-1}, respectively. Obviously, like in a previous study the nitrate removal in the CW-MFC with FN as anode and cathode material was significantly higher than that of the CW-MFC with CFF as electrode ($p < 0.05$) (Wang et al., 2017b). The data for NH_3-N and nitrate concentrations in the effluent samples of the four CW-MFC reactors indicate that nZVI increased the nitrogen removal.

It has been generally accepted that nitrification and denitrification are the main pathways for the removal of NH_3-N in wastewater treatment (Vymazal, 2007; Wallace et al., 2016). In this study, the removal efficiency for NH_3-N had a relatively low level. This may have resulted from the low concentration of DO in the wastewater limiting the nitrification. Although bacterial activities decreased with the reduced temperatures in winter, the removal of NH_3-N in the winter season was slightly higher than in the summer season. One possible reason may be that the DO concentration of the wastewater in the winter season was about 0.7 mg L^{-1} higher than in the summer season. In addition, the removal of nitrate in CW-MFC remained in the range of 85.0–92.5%. This suggests that the CW-MFC reactor possesses an advantage for nitrate removal from wastewater by simultaneous biological and chemical denitrification (Clauwaert et al., 2007; Vymazal, 2007). Compared with the bacterial communities in CW systems, the relative abundance of EAB was shown to be predominantly at the anode (Lu et al., 2015; Wang et al., 2017a). EAB are known to be able to desulphurize and to denitrify. Also the relative abundance of denitrifying bacteria (such as *Desulfovibrio* and *Dechloromonas*) in a CW-MFC with an anode amended with nZVI higher than in the corresponding CW-MFC (section 3.4). This may be the reasons, why the removal efficiency of nitrate in the FN-nZVI and CFF-nZVI reactors was slightly higher than in the FN and CFF systems.

3.4. Bacterial diversity and community distribution

To gain insight in the bacterial distribution responsible for the removal of nitrogen, phenanthrene and anthracene in the anodesphere of the CW-MFCs, high throughput sequencing analysis was used. As shown in Table S2, from the four samples were 17111-21703 high-quality sequences collected at the end of the experiment. The number of OTUs ranged from 1675 to 2858. ACE and Chao indexes were used to evaluate the richness of the bacterial community (Ebrahimi et al., 2010). The use of nZVI is enhancing the microbial richness of the CW-MFC with FN as anode material, while the richness of the bacterial community in the CW-MFC with a CFF anode amended with nZVI was lower than that of the CW-MFC with CFF. Shannon and Simpson estimators contain information about the richness and evenness of bacterial communities (Lu et al., 2015). The bacterial diversity evaluated by the Shannon estimator

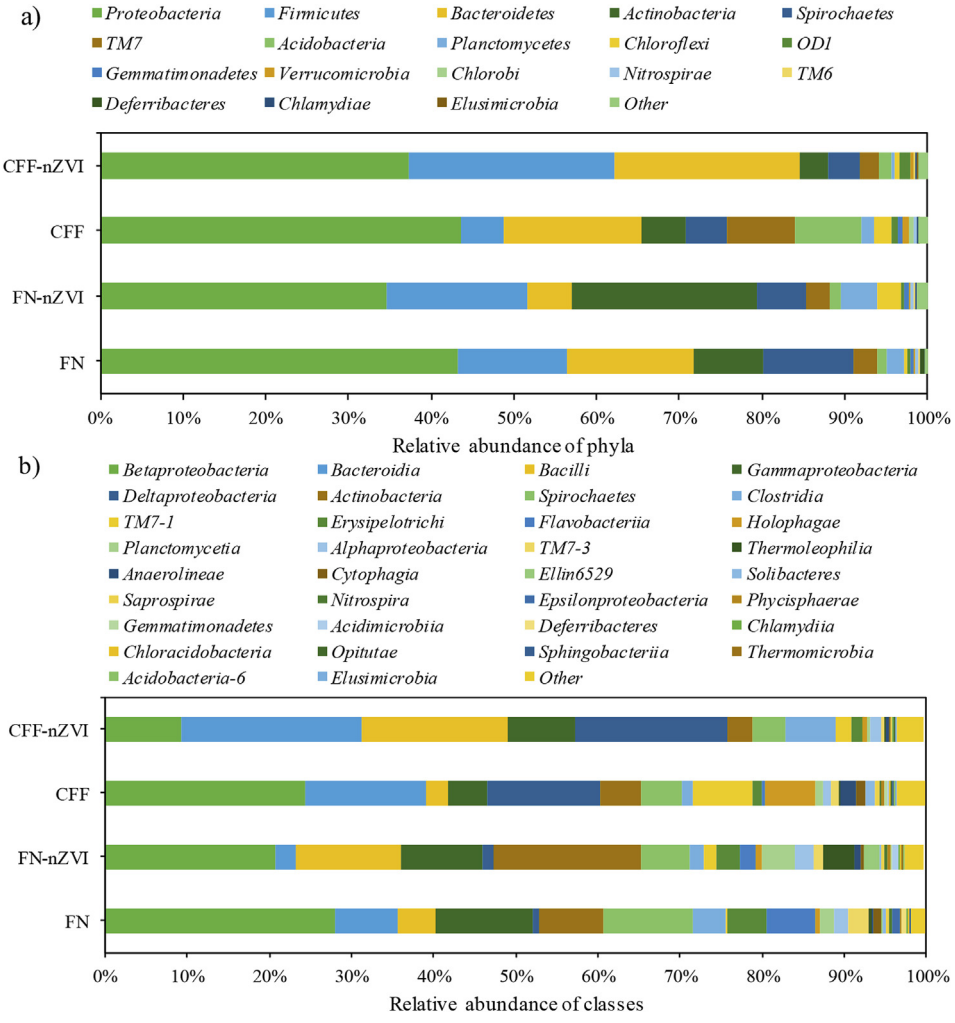

Fig. 6. The relative abundance of bacterial community at phylum (a) and class (b) level at anode of FN, FN-nZVI, CFF, and CFF- nZVI reactor.

indicated a similar trend like the ACE and Chao indexes. Obviously, the response of the bacterial communities to nZVI on FN or CFF anode material is significantly different.

At the phylum level [Fig. 6(a)], the main groups are *Proteobacteria* (average 39.7%), *Firmicutes* (average 15.2%), *Bacteroidetes* (average 14.9%), *Actinobacteria* (average 9.9%) and *Spirochaetes* (average 6.5%). Specifically, the relative abundance of the phylum *Proteobacteria* was in the CW-MFC with an anode without nZVI about 7.5% higher than in an CW-MFC with FN- nZVI or CFF- nZVI. However, the relative abundance of the phylum *Firmicutes* in the CW-MFC with FN or CFF as anode material was 4.0–20.0% lower than in the CW-MFC with nZVI. In addition, the relative abundance of *Bacteroidetes* and *Actinobacteria* in the FN-nZVI reactor was 5.3% and 22.6% higher than in FN system, respectively. The relative abundance of *Spirochaetes* in the four reactors were 10.9%, 5.9%, 5.0% and 4.0%, respectively. The bacterial community distribution at class level indicates the occurrence (average relative abundance>1%) of *Betaproteobacteria*, *Bacteroidia*, *Bacilli*, *Gammaproteobacteria*, *Deltaproteobacteria*, *Actinobacteria*, *Spirochaetes*, *Clostridia*, *Erysipelotrichi*, *Flavobacteriia*, *Holophagae*, *Planctomycetia*, *Alphaproteobacteria*, and *Thermoleophilia* as shown in Fig. 6(b). For the FN and CFF reactors, the relative abundance of *Bacteroidia*, *Bacilli*, *Actinobacteria* and *Deltaproteobacteria* anodes amended with nZVI an increase of abundance is noted. However, the relative abundance of some classes, like *Betaproteobacteria*, *Spirochaetes* and *Flavobacteriia*, became apparently reduced if anodes amended with nZVI were used.

The bacterial community distribution at genus level is presented in Fig. 7. A high abundance (average relative abundance>1.0%) of *Bacillus*, *Treponema*, *Propionicimonas*, *Paludibacter*, *Zoogloea*, *Pseudomonas, Desulfovibrio*, *Geobacter*, *Dechloromonas, Geothrix, Lactococcus, Uliginosibacterium* and *Cloacibacterium* was found. According to the distance matrix analysis, the bacteria at the anode in the FN and FN-nZVI reactors show a quite high similarity. However, the relative abundance of the genus *Bacillus*, *Clostridium*, *Paenibacillus* and *Ptopionivibtio* in the sample for CFF-nZVI was higher than for the CFF reactor. In addition, the CW-MFC of the anode with nZVI showed a higher relative abundance of the genus *Bacillus*, *Paludibacter*, *Desulfovibrio* and *Lactococcus* as compared with the corresponding CW-MFC system.

It has been demonstrated that the biodiversity of the bacterial community around a CFF anode in a CW-MFC is higher than in a FN reactor (Wang et al., 2017b). In addition, it is interesting that the application of nZVI to the anode causes a reduction of biodiversity in the CFF reactor and an enhancement in the FN system. This result is caused by the increased abundance of *Firmicutes* in FN reactor (Wang et al., 2017b). Finally, the richness of biodiversity in the CFF-nZVI system is lower than in the CFF reactor.

It has been reported that the EAB community is mainly consisting of the phyla *Proteobacteria* and *Firmicutes* (Lu et al., 2015). In this study the relative abundance of the *Proteobacteria* and *Firmicutes* respectively in FN-nZVI or CFF-nZVI is higher than in the corresponding CW-MFC system. The genus *Bacillus* is known to be electrogenic and able to degrade aromatic compounds and to

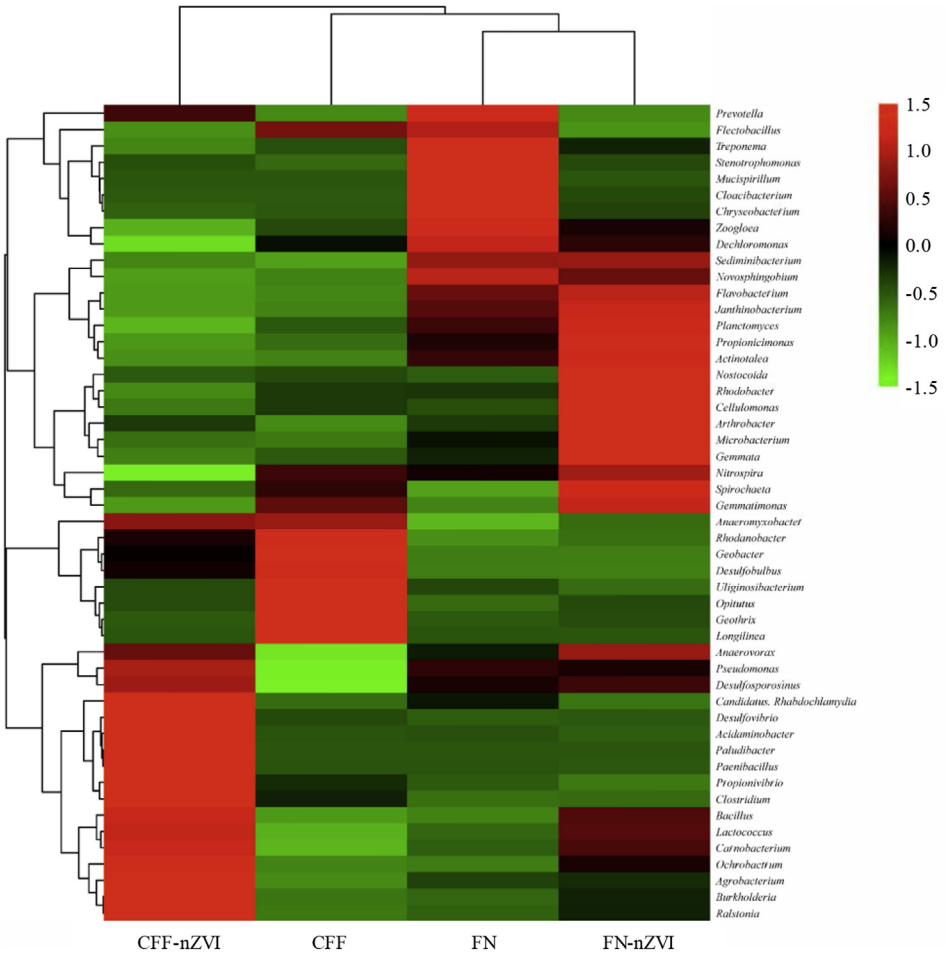

Fig. 7. Heat map graph of hierarchy cluster for the top 50 genera at anode of FN, FN-nZVI, CFF, and CFF- nZVI reactor.

excrete enzyme catalase (Baran et al., 2004; Kocabas et al., 2008). For the biodegradation of phenanthrene and anthracene, Fe^{3+} may be used as the catalyst to strengthen the activities of enzyme catalase (Spuhler et al., 2010). In addition, the enzyme dioxygenase contains an iron-sulfur centers (Fe_2S_3) (Ochiai, 1997), is also considered as an important enzyme to breakdown complex organic compounds. Therefore, the use of nZVI may have a positive effect on the metabolic activity and relative abundance of *Bacillus* species. A similar trend has also described for the genus *Paludibacter*, *Desulfovibrio* and *Lactococcus*. According to the distance matrix analysis the bacterial distribution in the four reactors was slightly different. This may have been an effect of the FN, which could have delivered trace elements conducive for the growth of some bacteria. This have a positive effect for adaptation of EAB and promote bioelectricity generation and biodegradation pathway of contaminant.

4. Conclusion

In the present study, we investigated the degradation pathway of phenanthrene and anthracene as model compounds for recalcitrant pollutants by CW-MFC is with anodes amended with or anodes without nZVI. The removal efficiency for phenanthrene and anthracene ranged from 88.5% to 96.4%. The results indicate that EAB microorganisms play an important role in the removal of these compounds. Measurements of phenanthrene and anthracene concentrations in the roots, stems and laminas of *T. orientalis* reveal that also phytoextraction and phytotransformation participate in the removal. Furthermore, bioelectricity generation and nitrogen removal were also promoted in CW-MFCs by the application of nZVI. The analysis of the bacterial community distribution indicates an enhancement of the abundance of *Bacillus*, *Paludibacter*, *Desulfovibrio* and *Lactococcus* species, who have a high degradation capability for recalcitrant pollutants.

Acknowledgements

This research is finished under the support of the National Nature Science Foundation of China (Grant Nos. 41673094, 51809116, 51679041, 91547209 and 41571037).

Appendix A. Supplementary data

Supplementary data to this article can be found online at https://doi.org/10.1016/j.watres.2018.11.075.

References

Baran, S., Bielińska, J.E., Oleszczuk, P., 2004. Enzymatic activity in an airfield soil polluted with polycyclic aromatic hydrocarbons. Geoderma 118 (3–4), 221–232.
Baron, S., 1996. Epidemiology–Medical Microbiology. University of Texas Medical Branch at Galveston.
Baxter-Plant, V., Mikheenko, I., Robson, M., Harrad, S., Macaskie, L., 2004. Dehalogenation of chlorinated aromatic compounds using a hybrid bioinorganic catalyst on cells of Desulfovibrio desulfuricans. Biotechnol. Lett. 26 (24), 1885–1890.
Cai, L., Zhang, H., Feng, Y., Wang, Y., Yu, M., 2018. Sludge decrement and electricity generation of sludge microbial fuel cell enhanced by zero valent iron. J. Clean. Prod. 174, 35–41.
Cheng, S., Liu, H., Logan, B.E., 2006. Increased power generation in a continuous flow MFC with advective flow through the porous anode and reduced electrode spacing. Environ. Sci. Technol. 40 (7), 2426–2432.
Clauwaert, P., Rabaey, K., Aelterman, P., De Schamphelaire, L., Pham, T.H., Boeckx, P., Boon, N., Verstraete, W., 2007. Biological denitrification in microbial fuel cells. Environ. Sci. Technol. 41 (9), 3354–3360.
Corbella, C., Guivernau, M., Vinas, M., Puigagut, J., 2015. Operational, design and microbial aspects related to power production with microbial fuel cells implemented in constructed wetlands. Water Res. 84, 232–242.
Doherty, L., Zhao, Y., Zhao, X., Wang, W., 2015a. Nutrient and organics removal from swine slurry with simultaneous electricity generation in an alum sludge-based constructed wetland Incorporating microbial fuel cell technology. Chem. Eng. J. 266, 74–81.
Doherty, L., Zhao, Y.Q., Zhao, X.H., Hu, Y.S., Hao, X.D., Xu, L., Liu, R.B., 2015b. A review of a recently emerged technology: constructed wetland - microbial fuel cells. Water Res. 85, 38–45.
Ebrahimi, S., Gabus, S., Rohrbach-Brandt, E., Hosseini, M., Rossi, P., Maillard, J., Holliger, C., 2010. Performance and microbial community composition dynamics of aerobic granular sludge from sequencing batch bubble column reactors operated at 20 °C, 30 °C, and 35 °C. Appl. Microbiol. Biotechnol. 87 (4), 1555–1568.
Fang, Z., Song, H.-l., Cang, N., Li, X.-n., 2015. Electricity production from Azo dye wastewater using a microbial fuel cell coupled constructed wetland operating under different operating conditions. Biosens. Bioelectron. 68, 135–141.
Fanning, J.C., 2000. The chemical reduction of nitrate in aqueous solution. Coord. Chem. Rev. 199 (1), 159–179.
Goldman, R., Enewold, L., Pellizzari, E., Beach, J.B., Bowman, E.D., Krishnan, S.S., Shields, P.G., 2001. Smoking increases carcinogenic polycyclic aromatic hydrocarbons in human lung tissue. Cancer Res. 61 (17), 6367–6371.
Gregoire, C., Elsaesser, D., Huguenot, D., Lange, J., Lebeau, T., Merli, A., Mose, R., Passeport, E., Payraudeau, S., Schuetz, T., 2009. Mitigation of agricultural nonpoint-source pesticide pollution in artificial wetland ecosystems–a review. In: Climate Change, Intercropping, Pest Control and Beneficial Microorganisms. Springer, pp. 293–338.
Hamdan, H.Z., Salam, D.A., Hari, A.R., Semerjian, L., Saikaly, P., 2017. Assessment of the performance of SMFCs in the bioremediation of PAHs in contaminated marine sediments under different redox conditions and analysis of the associated microbial communities. Sci. Total Environ. 575, 1453–1461.
Harada, T., Yatagai, T., Kawase, Y., 2016. Hydroxyl radical generation linked with iron dissolution and dissolved oxygen consumption in zero-valent iron wastewater treatment process. Chem. Eng. J. 303, 611–620.
Haritash, A.K., Kaushik, C.P., 2009. Biodegradation aspects of polycyclic aromatic hydrocarbons (PAHs): a review. J. Hazard Mater. 169 (1), 1–15.
Huang, L., Zhou, S., Jin, F., Huang, J., Bao, N., 2014. Characterization and mechanism analysis of activated carbon fiber felt-stabilized nanoscale zero-valent iron for the removal of Cr(VI) from aqueous solution. Colloid. Surface. Physicochem. Eng. Aspect. 447, 59–66.
Kocabas, D.S., Bakir, U., Phillips, S.E., McPherson, M.J., Ogel, Z.B., 2008. Purification, characterization, and identification of a novel bifunctional catalase-phenol oxidase from Scytalidium thermophilum. Appl. Microbiol. Biotechnol. 79 (3), 407–415.
Lei, A.-P., Hu, Z.-L., Wong, Y.-S., Tam, N.F.-Y., 2007. Removal of fluoranthene and pyrene by different microalgal species. Bioresour. Technol. 98 (2), 273–280.
Li, Y.F., Zhang, J.F., Zhu, G.B., Liu, Y., Wu, B., Ng, W.J., Appan, A., Tan, S.K., 2016. Phytoextraction, phytotransformation and rhizodegradation of ibuprofen associated with Typha angustifolia in a horizontal subsurface flow constructed wetland. Water Res. 102, 294–304.
Liu, S., Song, H., Wei, S., Yang, F., Li, X., 2014. Bio-cathode materials evaluation and configuration optimization for power output of vertical subsurface flow constructed wetland - microbial fuel cell systems. Bioresour. Technol. 166, 575–583.
Liu, Y., Zhang, Y., Quan, X., Li, Y., Zhao, Z., Meng, X., Chen, S., 2012. Optimization of anaerobic acidogenesis by adding Fe0 powder to enhance anaerobic wastewater treatment. Chem. Eng. J. 192, 179–185.
Logan, B.E., 2008. Microbial Fuel Cells. John Wiley & Sons.
Logan, B.E., Hamelers, B., Rozendal, R., Schröder, U., Keller, J., Freguia, S., Aelterman, P., Verstraete, W., Rabaey, K., 2006. Microbial fuel cells: methodology and technology. Environ. Sci. Technol. 40 (17), 5181–5192.
Lu, L., Xing, D.F., Ren, Z.J., 2015. Microbial community structure accompanied with electricity production in a constructed wetland plant microbial fuel cell. Bioresour. Technol. 195, 115–121.
Lv, T., Zhang, Y., Zhang, L., Carvalho, P.N., Arias, C.A., Brix, H., 2016. Removal of the pesticides imazalil and tebuconazole in saturated constructed wetland mesocosms. Water Res. 91, 126–136.
Nevin, K.P., Richter, H., Covalla, S.F., Johnson, J.P., Woodard, T.L., Orloff, A.L., Jia, H., Zhang, M., Lovley, D.R., 2008. Power output and columbic efficiencies from biofilms of Geobacter sulfurreducens comparable to mixed community microbial fuel cells. Environ. Microbiol. 10 (10), 2505–2514.
Ochiai, E.-I., 1997. The manifestation of evolutionary pressure in bioinorganic chemistry: principles and applications in bioinorganic chemistry - IX. J. Chem. Educ. 74 (3), 348.
Oon, Y.-L., Ong, S.-A., Ho, L.-N., Wong, Y.-S., Dahalan, F.A., Oon, Y.-S., Lehl, H.K., Thung, W.-E., Nordin, N., 2017. Role of macrophyte and effect of supplementary aeration in up-flow constructed wetland-microbial fuel cell for simultaneous wastewater treatment and energy recovery. Bioresour. Technol. 224, 265–275.
Pašková, V., Hilscherová, K., Feldmannová, M., Bláha, L., 2006. Toxic effects and oxidative stress in higher plants exposed to polycyclic aromatic hydrocarbons and their N-heterocyclic derivatives. Environ. Toxicol. Chem. 25 (12), 3238–3245.
Pilon-Smits, E., 2005. Phytoremediation. Annu. Rev. Plant Biol. 56, 15–39.
Qi, W.X., Liu, H.J., Pernet-Coudrier, B., Qu, J.H., 2013. Polycyclic aromatic hydrocarbons in wastewater, WWTPs effluents and in the recipient waters of Beijing, China. Environ. Sci. Pollut. Control Ser. 20 (6), 4254–4260.
Rabaey, K., Verstraete, W., 2005. Microbial fuel cells: novel biotechnology for energy generation. Trends Biotechnol. 23 (6), 291–298.

Rijnen, L., Bonneau, S., Yvon, M., 1999. Genetic characterization of the major lactococcal aromatic aminotransferase and its involvement in conversion of amino acids to aroma compounds. Appl. Environ. Microbiol. 65 (11), 4873–4880.
Robert, H.S., Friml, J., 2009. Auxin and other signals on the move in plants. Nat. Chem. Biol. 5 (5), 325.
Spuhler, D., Rengifo-Herrera, J.A., Pulgarin, C., 2010. The effect of Fe2+, Fe3+, H2O2 and the photo-Fenton reagent at near neutral pH on the solar disinfection (SODIS) at low temperatures of water containing Escherichia coli K12. Appl. Catal. B Environ. 96 (1–2), 126–141.
Villasenor, J., Capilla, P., Rodrigo, M.A., Canizares, P., Fernandez, F.J., 2013. Operation of a horizontal subsurface flow constructed wetland - microbial fuel cell treating wastewater under different organic loading rates. Water Res. 47 (17), 6731–6738.
Volbeda, A., Charon, M.-H., Piras, C., Hatchikian, E.C., Frey, M., Fontecilla-Camps, J.C., 1995. Crystal structure of the nickel–iron hydrogenase from Desulfovibrio gigas. Nature 373 (6515), 580.
Vymazal, J., 2007. Removal of nutrients in various types of constructed wetlands. Sci. Total Environ. 380 (1–3), 48–65.
Wallace, J., Champagne, P., Hall, G., 2016. Multivariate statistical analysis of water chemistry conditions in three wastewater stabilization ponds with algae blooms and pH fluctuations. Water Res. 96, 155–165.
Wang, J., Song, X., Wang, Y., Abayneh, B., Li, Y., Yan, D., Bai, J., 2016. Nitrate removal and bioenergy production in constructed wetland coupled with microbial fuel cell: establishment of electrochemically active bacteria community on anode. Bioresour. Technol. 221, 358–365.
Wang, J., Song, X., Wang, Y., Bai, J., Li, M., Dong, G., Lin, F., Lv, Y., Yan, D., 2017a. Bioenergy generation and rhizodegradation as affected by microbial community distribution in a coupled constructed wetland-microbial fuel cell system associated with three macrophytes. Sci. Total Environ. 607–608, 53–62.
Wang, J., Song, X., Wang, Y., Zhao, Z., Wang, B., Yan, D., 2017b. Effects of electrode material and substrate concentration on the bioenergy output and wastewater treatment in air-cathode microbial fuel cell integrating with constructed wetland. Ecol. Eng. 99, 191–198.
Wild, S.R., Jones, K.C., 1995. Polynuclear aromatic hydrocarbons in the United Kingdom environment: a preliminary source inventory and budget. Environ. Pollut. 88 (1), 91–108.
Yadav, A.K., Dash, P., Mohanty, A., Abbassi, R., Mishra, B.K., 2012. Performance assessment of innovative constructed wetland-microbial fuel cell for electricity production and dye removal. Ecol. Eng. 47, 126–131.
Yang, B., Xu, H., Wang, J., Song, X., Wang, Y., Li, F., Tian, Q., Ma, C., Wang, D., Bai, J., Sand, W., 2017. Bacterial and archaeal community distribution and stabilization of anaerobic sludge in a strengthen circulation anaerobic (SCA) reactor for municipal wastewater treatment. Bioresour. Technol. 244, 750–758.
Yu, B., Tian, J., Feng, L., 2017. Remediation of PAH polluted soils using a soil microbial fuel cell: influence of electrode interval and role of microbial community. J. Hazard Mater. 336, 110–118.
Yun, H., Liang, B., Kong, D.-Y., Cheng, H.-Y., Li, Z.-L., Gu, Y.-B., Yin, H.-Q., Wang, A.-J., 2017. Polarity inversion of bioanode for biocathodic reduction of aromatic pollutants. J. Hazard Mater. 331, 280–288.
Zhang, J., Zhang, Y., Quan, X., Liu, Y., An, X., Chen, S., Zhao, H., 2011. Bioaugmentation and functional partitioning in a zero valent iron-anaerobic reactor for sulfate-containing wastewater treatment. Chem. Eng. J. 174 (1), 159–165.
Zhang, X., Lin, S., Lu, X.-Q., Chen, Z.-l., 2010. Removal of Pb(II) from water using synthesized kaolin supported nanoscale zero-valent iron. Chem. Eng. J. 163 (3), 243–248.